Experimental Cell Research **278,** 31–44 (2002)
doi:10.1006/excr.2002.5544

Mouse Notch 3 Expression in the Pre- and Postnatal Brain: Relationship to the Stroke and Dementia Syndrome CADASIL

Nilima Prakash,*[,1] Emil Hansson,* Christer Betsholtz,† Thimios Mitsiadis,‡ and Urban Lendahl*[,2]

**Department of Cell and Molecular Biology, Medical Nobel Institute, Karolinska Institute, SE-171 77 Stockholm, Sweden; †Department of Medical Biochemistry, University of Göteborg, Medicinaregatan 9A, Box 440, SE-405 30 Göteborg, Sweden; and ‡Faculté d'Odontologie, Université de la Méditerranée, 27, boulevard Jean Moulin, 13385 Marseille Cedex 5, France*

Mutations in the human *Notch 3* gene cause the vascular stroke and dementia syndrome CADASIL (Cerebral Autosomal Dominant Arteriopathy with Subcortical Infarcts and Leukoencephalopathy) characterized by degeneration of vascular smooth muscle cells and multiple small infarcts in the white and deep gray matter of the brain. Here we have analyzed the expression pattern of the *Notch 3* gene in the pre- and postnatal mouse brain. Prenatal *Notch 3* expression is restricted to a scattered population of cells within the vessel wall of all major blood vessels in the developing embryo, including those that form the perineural vascular plexus. Expression in the postnatal brain is confined to a scattered cell population within the vessel wall of small to medium-sized penetrating arteries, which are the vessel type primarily affected in CADASIL patients. In contrast, no expression was observed in capillaries and veins. *Notch 3* is most likely expressed in a subset of vascular smooth muscle cells, and the expression pattern of one of the Notch ligands, *Serrate 1,* was very similar to that observed for *Notch 3.* The *Notch 3* expressing pattern was not significantly altered in platelet-derived growth factor B- (PDGF-B) deficient mouse embryos, demonstrating that *Notch 3* expression is not under direct control of PDGF-B. These data show that *Notch 3* expression is conserved between mouse and human and suggest that the mouse is a valid system for analysis of CADASIL.

Key Words: **CADASIL; dementia; Notch signaling; PDGF; stroke.**

INTRODUCTION

Vascular dementia is a medically important and multifaceted group of diseases. While many cases are sporadic, there is increasing evidence for inherited forms, which opens up a possibility to analyze the molecular mechanisms underlying vascular dementia. CADASIL (Cerebral Autosomal Dominant Arteriopathy with Subcortical Infarcts and Leukoencephalopathy) is one of the hereditary forms and results in multiple brain infarcts and dementia. It was originally described as a hereditary disease in 1977 [1] and later named CADASIL [2]. In 1996 the genetic cause of CADASIL was shown to be point mutations in the human Notch 3 gene [3].

The symptoms of CADASIL show a broad variability in affected families, and as a consequence of this, CADASIL is most likely underdiagnosed and often misdiagnosed [2]. Currently, there are more than 300 affected families described worldwide. More than 100 of those families are found in regions where more systematic DNA-based screening and diagnosis has been made, i.e. France, Scandinavia, and the UK. Prominent symptoms in CADASIL patients are recurring strokes due to ischemic brain infarcts, eventually leading to the dementia and the death of the patient [4, 5]. Clinical admittance is often in the 40s to 50s. However, magnetic resonance imaging scans reveal white matter abnormalities at earlier stages in still-asymptomatic CADASIL carriers, and migraine with aura, observed in approximately 30% of the patients, often begins as early as the teens [6, 8]. Histopathological analysis of CADASIL brains demonstrates a thickening of the vessel wall and narrowing of the lumen in certain arteries in the brain [7, 8]. In the thickened walls pathognomonic granular osmiophilic material (GOM) has accumulated in the extracellular space, vascular smooth muscle cells (VSMCs) have degenerated, and marked secondary fibrosis has occurred. The obliteration of the arteries and/or thrombosis eventually result in severe enough decrease in blood flow to cause infarctions, mainly in subcortical white matter and deep gray matter. Although symptoms in CADASIL are almost exclusively neurological, the vascular pathological changes in CADASIL patients are not only confined to the brain, but also observed in arteries of many organs, including skin, skeletal muscle, heart, and peripheral

[1] Present address: Research Group Wurst/ Molecular Neurogenetics, Max-Planck-Institute of Psychiatry, Kraepelinstrasse 2-10, D-80804 Munich, Germany.

[2] To whom correspondence and reprint requests should be addressed. Fax: +46 (8) 348135. E-mail: Urban.Lendahl@cmb.ki.se

0014-4827/02 $35.00

nerves [7, 8]. CADASIL is thus a systemic vasculopathy, although the effects of the disease are most severe in the brain. Findings in muscle and skin biopsies have suggested that arterial endothelial cells are also affected. Endothelial cells appear to shrink, detach from the basal lamina and the tight and gap junctions are disrupted. On the basis of these findings impaired permeability of vascular endothelium was proposed to play a role in VSMC destruction [8].

The human *Notch 3* gene was mapped to chromosome 19p13.1-13.2 [9], a region to which the CADASIL locus was subsequently localized [3]. Joutel *et al.* (1996) demonstrated that CADASIL was caused by mutations in the human *Notch 3* gene [3]. The *Notch 3* gene, like the three highly related *Notch 1, 2,* and *4* genes, encodes a large, single-pass transmembrane receptor [10]. The extracellular *Notch 3* domain contains 34 tandemly organized epidermal growth factorlike repeats (EGF repeats), and the intracellular domain harbors ankyrin repeats and a PEST domain ([10]; for review see [11, 12]). The mutations in the human *Notch 3* receptor gene in CADASIL patients show an interesting and unusual pattern. The vast majority of mutations reported to date are missense mutations in the EGF repeats of the extracellular domain [13, 14]. Most mutations are found in exons 3 and 4, corresponding to the first five EGF repeats, but others are located in a number of different EGF repeats. Furthermore, the missense mutations always involve a cysteine residue, i.e., either a cysteine is introduced or replaced, changing the number of cysteine residues in an EGF-repeat from six to either five or seven. Recently discovered small in-frame deletion mutations also specifically eliminate cysteine residues, further underlining the importance of these residues [14]. The relative clustering of mutations to exons 3 and 4 considerably facilitates screening for CADASIL mutations in patient materials.

Notch receptors function in a signaling pathway, which is an evolutionarily well conserved system for cell–cell communication. The signal is transmitted from transmembrane ligands (of the Delta or Serrate type) on neighboring cells to the *Notch* receptor. In response to ligand-activation, the *Notch* receptor is cleaved at the intracellular side, and the intracellular domain (IC) is translocated from the cytoplasm to the nucleus (for review see [15]). In the nucleus, the *Notch* IC interacts with a DNA-binding protein, RBP-Jκ, to activate transcription of downstream genes, the HES genes. Recent data have, however, shown that the intracellular aspect of *Notch* signaling in vertebrates is more complex and that the *Notch 3* IC appears to have a different role. The mammalian *Notch 1* and *2* ICs, as well as *Drosophila Notch* IC, activate transcription of HES genes, which can be referred to as the "classic" *Notch* signaling. *Notch 3* IC, in contrast, functions as a repressor of activation from *Notch 1* IC in certain contexts, during both CNS [16] and pancreas [17] development.

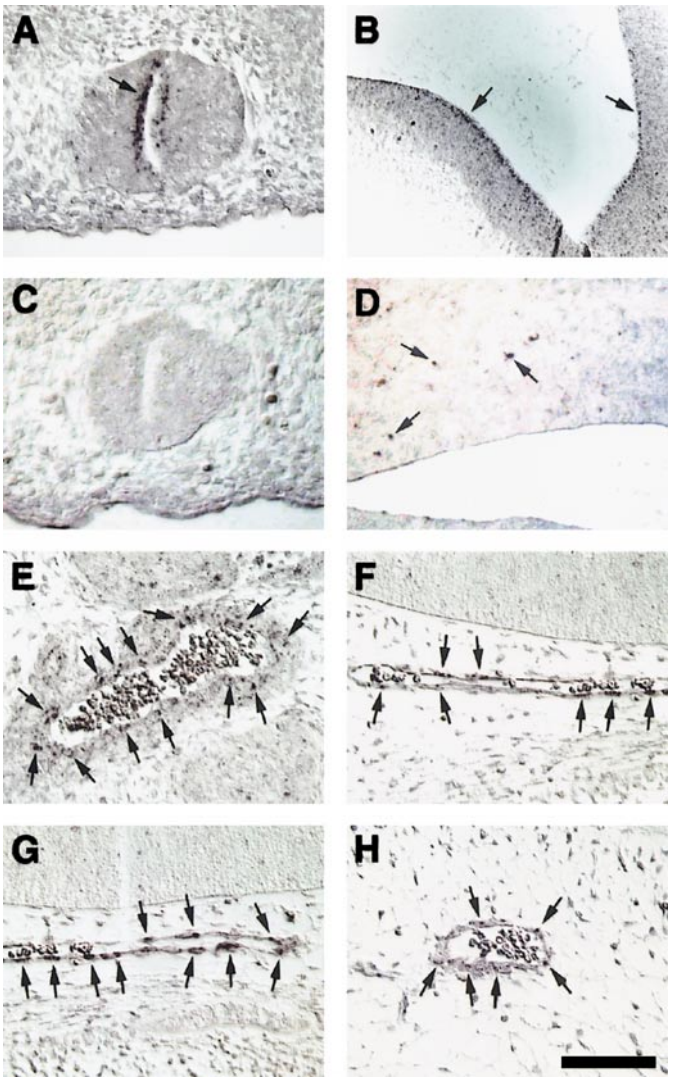

FIG. 1. *Notch 3* expression pattern in the E12.5 mouse embryo. Strong expression of mouse *Notch 3* is seen around the central canal of the spinal cord (A) and in the ventricular/subventricular zone of the midbrain (B), which is in agreement with previously published data [10, 21, 26, 38]. No signal was observed using a sense *Notch 3* probe (C), while a PDGF-B probe gave a distinct signal in the endothelium (D). At this stage, *Notch 3* is also expressed in a scattered population of cells (arrows) within the vessel wall of the aorta (E) or the perineural vascular plexus (F–H). (F and G) Longitudinal sections, and (H) cross section of major blood vessels forming part of the perineural plexus. Nonradioactive *in situ* hybridization on paraffin sections of a Dig-labeled mNotch 3 antisense riboprobe and subsequent detection using an anti-Dig/alkaline phosphatase conjugated antibody and NBT/BCIP enzymatic color reaction. Scale bar: 200 μm (B) and 100 μm (A, C–H).

Since a number of different organs and cell types are affected in CADASIL patients, it is of interest to precisely establish where the *Notch 3* gene is expressed

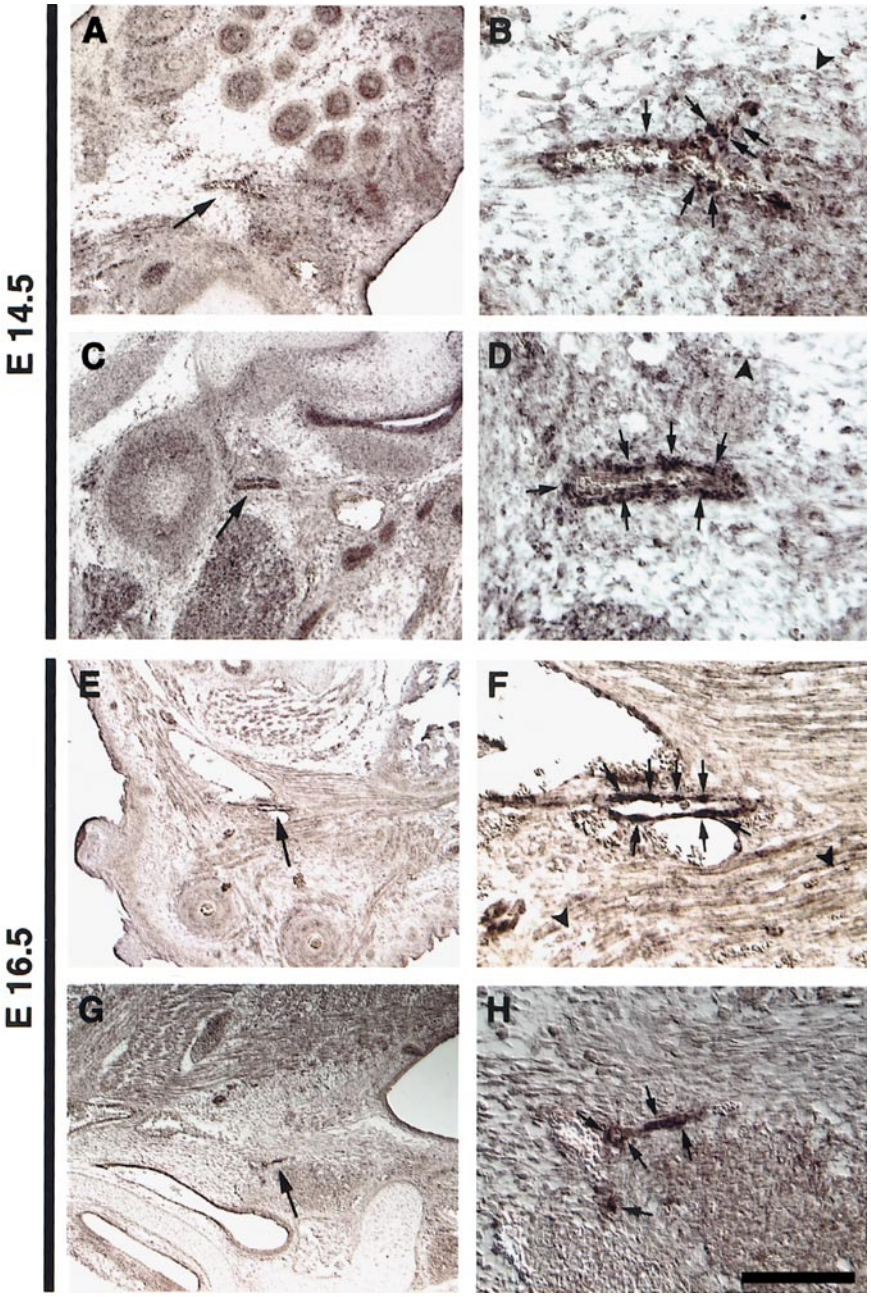

FIG. 2. Expression of *Notch 3* in perineural blood vessels of the head region in E14.5 and E16.5 mouse embryos. *Notch 3* is expressed in major arteries of the head in E14.5 (A and C) and E16.5 (E and G) embryos. Higher magnification (B, D, F, and H) of the arteries marked with arrows in A, C, E, and G reveals that *Notch 3* expression is not uniform but confined to a scattered population of cells within the vessel wall (arrows in B, D, F, and H). Note that no staining is seen in capillaries in close proximity to the stained vessels (arrowheads in B, D, and F). Nonradioactive *in situ* hybridization on paraffin sections of a Dig-labeled mNotch 3 antisense riboprobe and subsequent detection using an anti-Dig/alkaline phosphatase-conjugated antibody and NBT/BCIP enzymatic color reaction. Scale bar: 400 μm (A, C, E, and G) and 100 μm (B, D, F, and H).

during development. This would be important to identify the primary site of cellular changes, as *Notch* receptor functions are cell autonomous, i.e. take place in the cell expressing the receptor (for review see [18]). It has recently been shown that vascular smooth muscle cells in the human brain express the *Notch 3* receptor and that the levels of the ectodomain of the *Notch 3* receptor are elevated in CADASIL patients [19]. To establish how *Notch 3* is expressed during development and to learn whether the mouse would be a valid model for experimental genetic analysis of CADASIL, we have addressed how *Notch 3* is expressed at the mRNA

level during brain development in the pre- and postnatal mouse. We find that *Notch 3* expression is localized to a subset of cells in small to medium-sized penetrating arteries in the pre- and postnatal brain. These cells are most likely VSMCs, which suggests that the expression of *Notch 3* is well conserved between mouse and humans.

MATERIALS AND METHODS

Animals. Wild-type embryos and newborn pups were collected from timed pregnancies of CD-1 (E12.5), [C57B1/6J × CBA/J]F_1 (E14.5, E16.5, P0, P5, P11, and P15), and C57BL/6J (P20) mice. For pregnancy staging, the day of vaginal plug detection was designated Embryonic Day (E) 0.5. The day of birth was designated Postnatal Day (P) 0. Wild-type adult brains were obtained from C57BL/6J females. Platelet-derived growth factor B (PDGF-B)−/− and wild-type littermate embryos were genotyped as previously described [20].

Tissue preparation. Embryos and brains from P0, P5, P11, and P15 pups were dissected out under RNAse-free conditions in cold (4°C) phosphate-buffered saline [PBS; 5 mM NaH_2PO_4, 5mM Na_2HPO_4, 2.7 mM KCl, 137 mM NaCl (pH 7.4)]. Immediately after dissection, each embryo or brain was transferred to cold (4°C) fixative [4% paraformaldehyde; 4% sucrose; 5 mM EGTA; 2 mM $MgCl_2$ in PBS (pH 7.4)]. P20 and adult mice were perfused through the left ventricle of the heart with PBS followed by the fixative. Subsequently, brains were dissected out and transferred to fresh fixative. Embryos were fixed at room temperature (RT) for 6 h (E 12.5 and E 14.5) or overnight at 4°C (E16.5). P0 brains were fixed for 4 h at 4°C; P5, P20, and adult brains were fixed for 6–7 h at RT; P11 and P15 brains were fixed overnight at 4°C. Embryos and brains were washed 4× 15 min in PBS at RT, dehydrated through a graded ethanol series [2× 15 min (RT) and overnight (4°C) in 70% and 4× 30 min in each 95 and 100% ethanol at 4°C], and cleared in xylene (2× 30 min). The tissues were transferred to melted paraffin wax [Histowax (low melting point), Histolab, Göteborg, Sweden] and incubated 1 h and overnight at 58°C. Embryos and brains were embedded in fresh paraffin and kept at 4°C until sectioning. Sections (5–8 μm) were obtained on a Mikron HM 360 microtome (Mikron, Walldorf bei Heidelberg, Germany). Sections were mounted on Superfrost Plus (Menzel Gläser, Braunschweig, Germany) slides and dried at 37–40°C for at least 1 day. All sections were stored at 4°C in air-tight containers until use.

In situ hybridization. Immediately before use, sections were kept for 1 h at RT. Sections were dewaxed in xylene (2× 5 min), rehydrated in a graded ethanol series (2× 5 min 100%, 1 min each 95%, 70%, 50% ethanol), and washed 2× 5 min in PBS, all at RT. Sections were treated with Proteinase K [10 μg/ml in TE-Buffer (pH 7.5) preheated at 65°C] for 10–15 min at 37°C. The Proteinase K treatment was stopped in 0.2% glycine in PBS (5 min at RT), followed by a postfixation step in the same fixative as indicated above (10 min at RT). Subsequently, slides were washed 2× 5 min in PBS; dehydrated in 70, 95, and 100% ethanol (1 min each); air-dried; covered with HybriWell chambers (Surgipath, Richmond/IL); and immediately processed for hybridization of the probe. Digoxigenin- (Dig) labeled antisense and sense riboprobes for mouse *Notch 3* (mNotch 3), mSerrate-1, mDelta-like 1 [21], and PDGF-B [22] were synthesized from linearized plasmid cDNA templates using T3, T7, and SP6 RNA polymerases and following the manufacturer's instructions (Roche, Mannheim, Germany). The corresponding ^{35}S-labeled riboprobes were synthesized using 100 μCi ^{35}S-labeled α-CTP and following standard procedures [23]. Integrity of all riboprobes was routinely checked on agarose gels and labeling efficiency was routinely controlled on dot blots (using a Dig-labeled standard, Roche, Mannheim, Germany) or by scintillation counting. The amount of probe used in the *in situ* hybridization experiments was adjusted to a known standard, while all other parameters were left constant. Thus, although the method employed does not allow for quantitative measurements, we aimed at establishing a relative comparison of signal intensity between the different developmental stages that were analyzed in this study. Sections were hybridized for at least 20 h at 65°C (45°C for the mDelta-like 1 probes) in hybridization buffer [50% formamide, 5× SSC, 5× Denhardt's, 0.2% sodium dodecyl sulfate (SDS), 200 μg/ml heparan sulfate, 100 μg/ml poly(A) homopolymer, 250 μg/ml yeast tRNA, 250 μg/ml herring sperm DNA, and 10 mM dithiothreitol (DTT) in case of radioactive probes]. Probe concentration was as follows: Dig-labeled mNotch 3, mSerrate-1, and mDelta-like 1 antisense and sense probes: 1 μg/ml; Dig-labeled PDGF-B antisense and sense probes: 2 μg/ml; ^{35}S-labeled probes: 2×10^7 cpm/ml. After hybridization, sections were washed under stringent conditions in 1× SSC [150 mM NaCl and 15 mM Tris–Na citrate (pH 7.0)], 0.1% SDS for 30 min at RT and 60 min at 60°C, and in 0.1× SSC, and 0.1% SDS for 1× 60 min and 1× 30 min at 60°C. Dithiothreitol (10 mM) was added to each of these washes when radioactive probes had been used. Subsequently, sections hybridized with Dig-labeled riboprobes were further processed for immunohistochemical detection of the probe using an anti-Dig/alkaline phosphatase-conjugated antibody (1:500; Roche), followed by the color reaction with NBT/BCIP according to standard protocols (Roche). Sections were briefly rinsed in destilled water (Aq. dest.) and embedded in glycerol gelatin. Sections hybridized with ^{35}S-labeled probes were rinsed twice in 2× SSC (5 min each) at RT and dehydrated in a graded alcohol series (70 and 95% ethanol, 1 min each; 2× 5 min in 100% ethanol). Slides were dried overnight at RT and dipped in Kodak NTB-2 (Kodak, Rochester, NY) emulsion. Sections were exposed for 7 weeks at 4°C, developed in Kodak D19 developer, and fixed in Kodak fixative according to the manufacturer's instructions; cleared in 50% ethanol at 55°C for several days; dehydrated in 70, 95, and 100% ethanol (3 min each); rinsed in xylene for 2× 5 min; and embedded in Pertex (Histolab, Gothenburg, Sweden). Sections were viewed with a Nikon Eclipse E800 (Nikon, Tokyo, Japan) microscope using interference contrast optics and digital images were obtained with a SPOT camera and attached software (SPOT Software v2.2; Diagnostic Instruments Inc., Sterling Heights/MI).

Immunohistochemistry. Paraffin sections were obtained as indicated above. Sections that were processed for detection of smooth muscle α-actin (α-SMA) were dewaxed in xylene (1× 10 and 1× 5 min), rehydrated in a graded alcohol series (2× in 100 and 95%, and 1× in 70 and 50%, 3 min each), rinsed 3× 5 min in Aq. dest. and steamed for 2× 5 min in hot citric acid [10 mM citric acid (pH 6.0)] in a microwave oven. Sections that were processed for detection of platelet-endothelial cell adhesion molecule-1 (PECAM-1) were incubated at 56°C for 45 min, dewaxed, and rehydrated as indicated above; rinsed in Aq. dest. (3× 5 min); and treated for 20 min with trypsin (Life Technologies, Carlsbad, CA) at 37°C. Sections that were processed for detection of *Notch 3* extracellular domain [24] were dewaxed and rehydrated as indicated above and rinsed in Aq. Dest (3× 5 min). All slides were washed 3× 5 min in PBS after the corresponding pretreatment. Endogenous peroxidase activity was subsequently blocked by incubation in 3% H_2O_2 in methanol for 10 min. Slides were rinsed for 2× 1 min in Aq. dest. and 3× 5 min in PBS. Sections were incubated for 30 min in TNB blocking buffer [0.5% ‰ blocking reagent; 100 mM Tris–HCl (pH 7.5) 150 mM NaCl; NEN Life Sciences, Boston, MA] at RT and with the corresponding primary antibodies (rat antimouse PECAM-1 1:500, a kind gift from Dr. U. Eriksson; monoclonal α-SMA 1:400, Sigma, St. Louis, MO) in TNB buffer or rabbit antimouse *Notch 3* extracellular domain 1:400 [24] overnight at 4°C. Subsequently, all sections were processed for visualization of the corresponding epitopes with the Renaissance TSA-Indirect kit (NEN Life Sciences) according to protocols supplied by the manufacturer, using a biotinylated donkey antirat secondary

antibody immunopurified from mouse IgGs (1:300), a biotinylated donkey antimouse secondary antibody immunopurified from rat IgGs, or a donkey antirabbit secondary antibody (both at 1:100) (from Jackson ImmunoResearch Laboratories Inc., West Grove, PA). Sections were incubated in 0.5 mg/ml 3.3′-diaminobenzidine + 0.1% H_2O_2, and the color reaction was left to develop for 5 to 20 min. Slides were briefly washed in Aq. dest., dehydrated in graded ethanol, rinsed in xylene, mounted in Pertex, and visualized in a Nikon Eclipse E800 microscope as previously described.

Reverse transcription–polymerase chain reaction. Human fetal (16–32 weeks) and adult (37–60 years) brain polyA$^+$ RNA was purchased from Clontech (Palo Alto, CA). Synthesis of random hexamer-primed cDNA was performed using the First-Strand cDNA Synthesis kit (Amersham Pharmacia Biotech, Uppsala, Sweden) according to the manufacturer's protocol. Amplification of a 401-bp fragment of human *Notch 3* cDNA (GenBank accession number U97669) was performed using the following primer pair: forward primer, 5′-CTTCTCACTGCACAAGGACG-3′; reverse primer, 5′-CCTCATCCTCTTCAGTTGGC-3′; corresponding to positions 5115–5134 and 5496–5515 (accession number U97669), respectively. As positive control, amplification of a 308-bp fragment of human β-actin cDNA (GenBank Accession number X00351/J00074/M10278) was performed using the following primer pair: forward primer, 5′-ACTCTTCCAGCCTTCCTTCC-3′; reverse primer, 5′-CATACTCCTGCTTGCTGATCC-3′; corresponding to positions 821–840 and 1108–1128 (accession number X00351), respectively. Amplifications were performed using *Taq* DNA polymerase (MBI Fermentas, St. Leon-Rot, Germany) under the following conditions: 1.5 mM $MgCl_2$, 200 μM each dNTP, 1 μM of each primer, and 1 μl from the cDNA-synthesis reactions or water controls. Cycling parameters were as follows: denaturation step, 30 s at 92°C; annealing, 90 s at 56°C; and primer extension for 90 s at 72°C in a total of 36 cycles. In the first cycle, the denaturation step was extended to 60 s, and in the last cycle, the extension step lasted 3 min. The PCR products were separated on a 2.5% low-melting-point agarose gel and blotted onto a Hybond-N nylon membrane (Amersham, Piscataway, NJ). The blotted PCR products were subsequently hybridized with a [^{32}P]γ-ATP end-labeled oligonucleotide 5′-AACCAGATGGTGTTGAGTCCACTGACG GCAATCCACAGCCTCCTCAGC-3′ corresponding to positions 5299–5346 (accession number U97669) of human *Notch 3* cDNA (20,000 cpm/ml probe in high-stringency hybridization buffer, 200 mM Na-phosphate; 7% SDS; 1 mM EDTA; 1% BSA; 15% formamide). After hybridization, the membrane was washed in high-stringency washing buffer (0.2× SSC, 0.1% SDS) for 4× 30 min at 60°C and exposed on a Super RX Fuji Medical X-Ray film (Fujifilm, Stockholm, Sweden) for 30 min.

RESULTS

Notch 3 Expression in the Developing Mouse Embryo

In order to study the expression pattern of the mouse *Notch 3* gene in the pre- and postnatal mouse brain with good cellular resolution, we used a nonradioactive *in situ* hybridization protocol with Dig-labeled riboprobes. The specificity and sensitivity of this protocol were first tested by comparing the observed staining pattern with previously published results. *Notch 3* expression was seen in scattered cells around the central canal in the developing spinal cord (Fig. 1A) and in the ventricular/subventricular zone of the midbrain (Fig. 1B) of the E12.5 mouse embryo. This expression pattern is in good keeping with previous observations in mouse and rat embryos [10]. We therefore conclude that our *in situ* hybridization protocol is sensitive enough to detect expression of the *Notch 3* gene in a similar fashion as previously described with other methods. Furthermore, specificity of the *Notch 3* signal was routinely established by hybridization of adjacent tissue sections with a sense probe (negative control) that gave no staining in all cases studied (Fig. 1C). A PDGF-B antisense riboprobe that detects PDGF-B expression in endothelial cells of immature capillaries and arteries/arterioles [20] was routinely included in the hybridization protocol as a positive control (Fig. 1D).

In the E12.5 mouse embryo, we observed a scattered Notch 3 expression within the vessel wall of the aorta (Fig. 1E) and along the major blood vessels that form part of the perineural vascular plexus (Figs. 1F–1H). It should be noted that expression is not continuous within the vessel wall but seems to be rather restricted to a subset of vascular mural cells (arrows in Figs. 1E–1H). No expression of *Notch 3* can be detected at this stage in newly forming vessels in the parenchyma of the developing brain (data not shown).

A similar expression pattern persists also at later stages of mouse embryonic development. At E14.5 and E16.5, high expression of *Notch 3* was seen in cells within the wall of the aorta (data not shown), and a lower signal was detected in perineural blood vessels in the head region, which eventually will give rise to the carotid and other cranial arteries (Figs. 2A, 2C, 2E, and 2G). Analysis of these vessels at higher magnification reveals that *Notch 3* expression was not uniformly distributed within the vessel wall, but rather confined to a scattered cell population (arrows in Figs. 2B, 2D, 2F, and 2H). Expression of the *Notch 3* gene was not detected in the smaller vessels that penetrate into the developing brain or in the numerous brain capillaries in any of the sections and embryos studied (arrowheads in Figs. 2B, 2D, and 2F). In conclusion, *Notch 3* is expressed in a scattered cell population within the wall of all major blood vessels of the developing mouse embryo.

Notch 3 Expression in the Postnatal and Adult Mouse Brain

We next analyzed *Notch 3* expression in the mouse brain at early postnatal and adult stages. We could detect no staining using Dig-labeled probes in the P0 mouse brain (data not shown). Staining intensity gradually increased in the course of early postnatal development up to P15 and decreased thereafter at P20. Expression of *Notch 3* in the P5 (Figs. 3A–3C), P11 (Figs. 3D–3F) and P15 (Figs. 3G–3I) mouse brain was strictly associated with small to medium-sized penetrating arteries in superficial (Figs. 3A, 3B, 3F, 3G, and 3H) or deeper (Figs. 3C–3E and 3I) cortical areas, also extending into the developing white matter. No staining was seen in arterioles or capillaries in proximity to

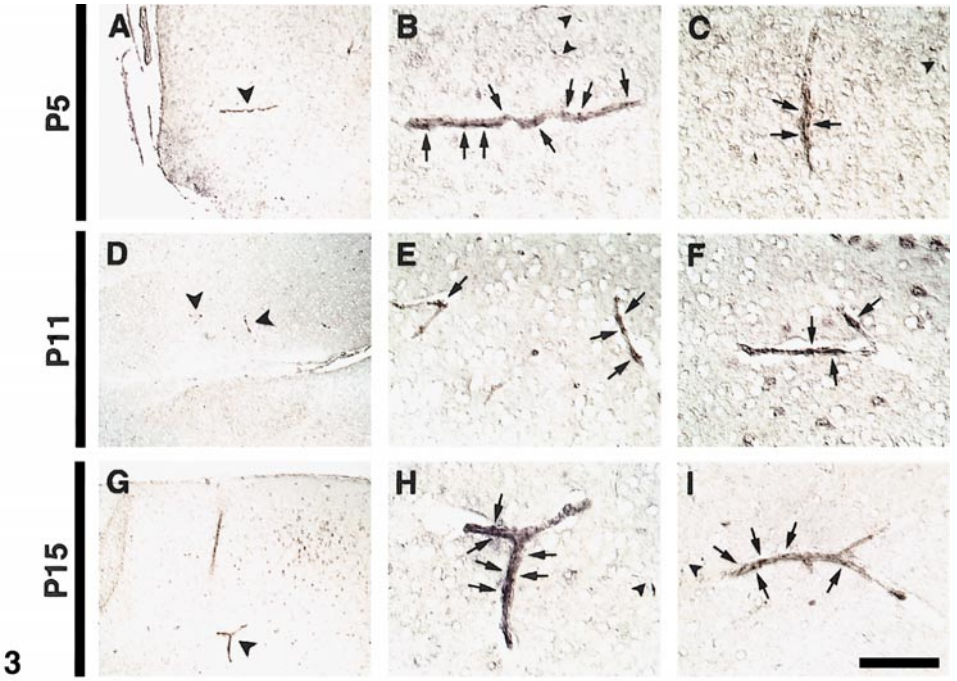

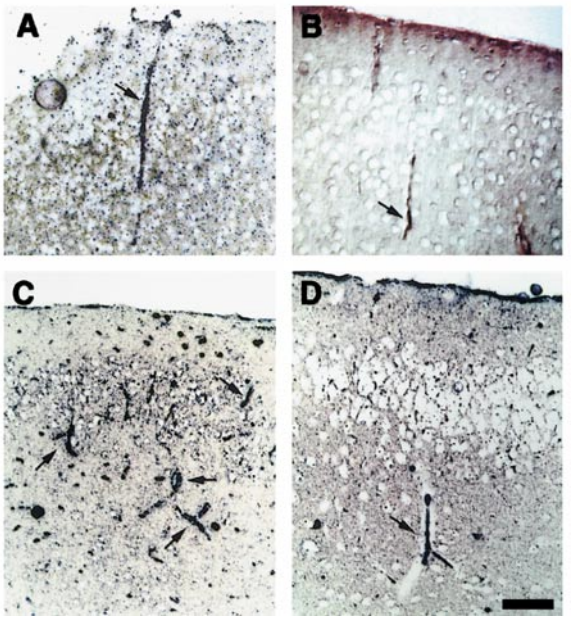

FIG. 3. Expression of *Notch 3* in the early postnatal mouse brain. Staining is seen in small to medium-sized penetrating arteries of superficial (A, B, F–H) or deeper (C–E and I) cortical areas of the mouse brain on postnatal days 5 (A–C), 11 (D–F), and 15 (G–I). (A, D, and G) Overview showing the location of stained arteries (arrowheads) depicted at higher magnification in B, E, and H, respectively. Note the punctuated distribution of the stain over the vessel wall (arrows in B, C, E, F, H, and I). No staining was seen in capillaries in close proximity to the stained vessels (arrowheads in B, C, H, and I). Nonradioactive *in situ* hybridization on paraffin coronal sections of a Dig-labeled mNotch 3 antisense riboprobe and subsequent detection using an anti-Dig/alkaline phosphatase conjugated antibody and NBT/BCIP enzymatic color reaction. Scale bar: 400 μm (A, D, and G) and 100 μm (B, C, E, F, H, and I).

FIG. 4. Expression of *Notch 3* in penetrating arteries of the P20 and adult mouse brain. The silver grain pattern after radioactive *in situ* hybridization on paraffin sections with a ^{35}S-labeled mNotch 3 antisense riboprobe was detected using darkfield optics and superimposed on the brightfield view of the same area of the section (A, C, and D). Comparison between radioactive (A) and nonradioactive (B) *in situ* hybridization using a ^{35}S-labeled and a Dig-labelled mNotch 3 antisense riboprobe, respectively. Note the similarity in staining using the two protocols. Several stained small to medium-sized penetrating arteries are seen in the P20 brain (black arrows in C), while a staining was observed only occasionally on medium-sized penetrating arteries in the adult brain (black arrows in D). The intense signal seen along the perineural vascular plexus is produced by the accumulation of erythrocytes within the vessel lumen that cause a similar light scattering as the silver grains. Scale bar: 100 μm.

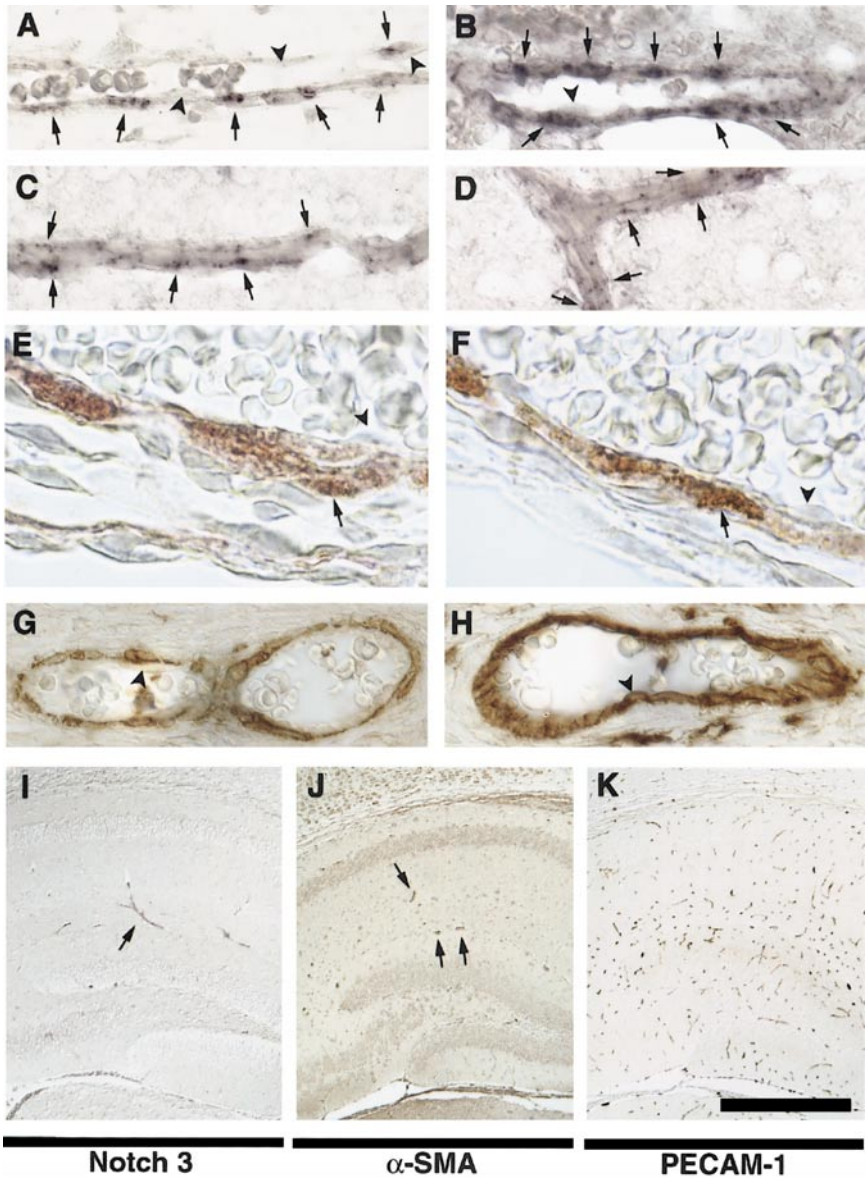

FIG. 5. Comparison of the mouse *Notch 3* expression pattern with that of vascular smooth muscle and endothelial cell markers. High-power magnification of *Notch 3* expression in vessels: A (E12.5, from vessel shown in Fig 1E); B (E16.5, from Fig. 2H); C (P5, from Fig. 3B); and D (P15, from Fig. 3H). Note that the staining is confined to a subset of cells within the vessel wall (arrows) that appears to be morphologically distinct from endothelial cells (arrowheads). *Notch 3* immunohistochemistry of the aorta wall from an E14.5 embryo (E and F) reveals *Notch 3* immunoreactivity in VSMCs (arrows) but not in endothelial cells (arrowheads). For comparison, in a head artery of a E14.5 mouse embryo (G) the distribution of VSMCs is shown by expression of the VSMC marker α-SMA, and in H the distribution of endothelial cells by staining for PECAM-1, an endothelial cell marker. In addition, at low-power magnification, the overall expression pattern for *Notch 3* (I) resembles the staining pattern of α-SMA in VSMCs (J), with only major blood vessels being stained (arrows), and is clearly distinct from the staining pattern for PECAM-1 on endothelial cells (K). Semiadjacent sections of the hippocampal area in a P15 mouse brain (I, J, and K). *Notch 3* mRNA was detected by *in situ* hybridization with a Dig-labeled antisense riboprobe and subsequent anti-Dig/alkaline phosphatase catalyzed enzymatic color reaction (NBT/BCIP) (A-D, I). α-SMA (J), PECAM-1 (K), and Notch 3 (E and F) were detected with the corresponding primary antibody and subsequent visualization using the Tyramid Signal Amplification kit as described under Material and Methods. Scale bar: 82 μm (A, B, C, D, G, and H), 40 μm (E and F), and 500 μm (I, J, and K).

the stained vessels (arrowheads in Figs. 3B, 3C, 3H, and 3I). Consistent with our observations at the prenatal stages, expression was not uniformly distributed over the vessel wall, but concentrated to a subset of mural cells (note the punctuated distribution of the staining in all vessels shown; arrows in Figs. 3B, 3C, 3E, 3F, 3H, and 3I). Some of the *Notch 3*-expressing vessels are branching arteries, and here either both

branches (Figs. 3F and 3H) or only one of the two branches (Fig. 3I) expressed *Notch 3*. It should be noted that expression of *Notch 3* was not seen in veins.

We could not detect *Notch 3* expression in the P20 and adult mouse brain using the nonradioactive probe, most likely because the expression levels were too low at these stages. We therefore used a more sensitive radioactive *in situ* hybridization protocol with ^{35}S-labeled probes for these stages. Comparison between the staining pattern obtained with a Dig-labeled *Notch 3* riboprobe and the autoradiographic pattern using an ^{35}S-labeled probe in a P15 brain revealed no obvious differences (compare Figs. 4A and 4B), demonstrating the specificity of the ^{35}S-labeled probe. Using this probe, we found that *Notch 3* was expressed in small penetrating arteries of the P20 (Fig. 4C) and adult (Fig. 4D) mouse brain, i.e., the same sites of expression as in earlier postnatal stages. In the adult brain, *Notch 3* expression also appeared to be associated with the vessel wall periphery, although this cannot be established conclusively because of the scattering of silver grains over the vessel.

Comparison of the Notch 3 mRNA Expression Pattern with Markers for Endothelial and Vascular Smooth Muscle Cells in the Pre- and Postnatal Mouse Brain

We next wanted to establish which cell type the scattered *Notch 3*-expressing cells represent. High-power magnifications of stained vessels in the embryonic head region showed that *Notch 3* is expressed in a subpopulation of cells that lie within the vessel wall (arrows in Figs. 5A and 5B) but not in morphologically identifiable endothelial cells immediately adjacent to the vessel lumen (arrowheads in Figs. 5A and 5B). Furthermore, *Notch 3* staining seems to be preferentially associated with the vessel periphery in postnatal brains (arrows in Figs. 5C and 5D). In addition, we never detected *Notch 3* expression in the brain capillaries (data not shown), which consist of an endothelial tube with associated pericytic processes, but lack smooth muscle cells [20]. By immunohistochemistry, using an anti-*Notch 3* antiserum, we also observed *Notch 3* immunoreactivity in VSMCs in the E14.5 aorta (arrows in Figs. 5E and 5F), but not in endothelial cells (arrowheads in Figs. 5E and 5F).

These observations argue that *Notch 3* is expressed in VSMCs but not in endothelial cells. To test this hypothesis further, we compared the *Notch 3* expression pattern with that of markers for VSMCs and endothelial cells on semiadjacent sections. At high-power magnification, the *Notch 3* mRNA expression pattern (Figs. 5. A–D) is clearly similar to the staining pattern for the VSMC marker α-SMA (Fig. 5G), but not to the pattern observed for the endothelial cell marker PECAM-1 (Fig. 5H). It should be noted that in a given vessel, the number of α-SMA-expressing cells almost always exceeded the number of *Notch 3*-expressing cells (compare Figs. 5A and 5G), suggesting that only a proportion of VSMCs express *Notch 3*, although the number of expressing cells could only be compared in adjacent sections. Moreover, at lower magnification, the α-SMA pattern (Fig. 5J) was very similar to the *Notch 3* expression pattern (Fig. 5I), i.e., only major blood vessels of the perineural vascular plexus in the embryo or small to medium-sized penetrating arteries in the postnatal brain are labeled (arrows). In contrast, the staining pattern for PECAM-1 (Fig. 5K) is much more elaborate and clearly distinct from that of *Notch 3*. Taken together, these data support the notion that mouse *Notch 3* is expressed in a subset of VSMCs of the arterial vessel wall. The notion that *Notch 3* is expressed in VSMCs in the mouse receives support from recent data from mouse E14.5 aorta [25]. Furthermore, expression of the human *Notch 3* receptor has been localized to VSMCs in adult CADASIL and control brains [19].

Notch 3 Expression in PDGF-B−/− Mouse Embryos

VSMC development is partly controlled by PDGF signaling and to learn whether the *Notch 3*-expressing cells depend on PDGF signaling, we analyzed *Notch 3* expression in PDGF-B-deficient mouse embryos. PDGF-B−/− mouse embryos display a nearly complete loss of pericytes from brain capillaries and a significant reduction in the number of VSMCs in the larger vessels [20, 22]. Furthermore, no α-SMA-positive VSMCs are found within the brain of PDGF-B−/− embryos, but vessels from the perineural vascular plexus still exhibit a partial VSMC coat [20]. The mutant embryos also exhibit secondary changes such as capillary dilation and rupture, causing their premature death around birth. As shown in Fig. 6, no obvious difference in the *Notch 3* expression pattern could be detected in the cranial arteries of an E14.5 PDGF-B−/− embryo compared to a wild-type littermate. We observed, however, that the extent of Notch 3 staining was somewhat reduced in the wall of the larger vessels in the body of the knock-out embryo (compare Figs. 6A and 6B), but less obvious so in cranial arteries (compare Figs. 6C and 6D). We thus conclude that the changes in *Notch 3* expression are consistent with the VSMC hypoplasia observed in small and medium-sized arteries in PDGF-B-deficient embryos [20]. Furthermore, *Notch 3* expression appears not to be exclusively dependent on PDGF-B signaling, since expression is still observed in PDGF-B−/− embryos.

Comparison of Notch 3 Expression with Serrate (Jagged) 1 and Delta-like 1 (Dll1) Expression in the Pre- and Postnatal Mouse Brain

To learn more about the expression of putative *Notch 3* ligands in the pre- and postnatal mouse brain, we analyzed the expression patterns of *Serrate (Jagged) 1* and *Delta-like 1 (Dll-1)*. We first demonstrated that the Dig-labeled riboprobe detected *Serrate 1* expression in a similar fashion as has previously been described using other hybridization protocols. Scattered cells in the midbrain region of an E12.5 mouse embryo expressed *Serrate 1* (Fig. 7A), and intense staining was seen in the developing kidney tubules in an E14.5 embryo (Fig. 7B), which is in agreement with previously published data [21, 26].

From E12.5 to E16.5, *Serrate 1* expression was observed in all major blood vessels of the body (data not shown) and head region (Figs. 7C and 7E). *Serrate 1* expression persisted into postnatal stages, where it was confined to vessels of the perineural vascular plexus and to small to medium-sized penetrating arteries of the brain (Figs. 7G and 7I). Although we could not detect expression of *Serrate 1* in the adult mouse brain using the Dig-labeled riboprobe, we clearly saw an autoradiographic signal on the same type of arteries using a ^{35}S-labeled riboprobe (data not shown). It should be noted here that we never observed expression of *Serrate 1* in small arterioles, capillaries or veins of the brain (arrowhead in Fig. 7K) or other body regions, i.e., the *Serrate 1* pattern was very similar to that of *Notch 3*. High-power magnification of the stained vessels revealed that *Serrate 1* expression is not uniform but confined to a scattered population of cells within the vessel wall (arrows in Figs. 7D, 7F, 7H, and 7K). The site of *Serrate 1* expression overlapped with the α-SMA-positive cells in the vessel wall (data not shown) and was absent in morphologically distinct endothelial cells (arrowheads in Fig. 7F). Furthermore, *Serrate 1* expression appeared to be unaffected in PDGF-B$-/-$ mouse embryos (compare Figs. 7L and 7M). This leads us to conclude that *Serrate 1* is expressed in VSMCs of embryonic and postnatal arterial vessels that may belong to the same PDGF-B-independent progenitor pool in which *Notch 3* is expressed. However, we cannot establish at this point whether *Serrate 1* and *Notch 3* are expressed in the same or in neighboring cells. In contrast to the staining pattern seen for *Notch 3*, the staining intensity after hybridization with a *Serrate 1* probe appeared to decline continuously after birth (data not shown).

We could not detect *Dll-1* expression in blood vessels of the embryo or postnatal/adult brain (data not shown). The lack of *Dll-1* expression in adult brain is in keeping with a previous report [27], but is in contrast to a recent observation, where a *lac*Z gene "knock-in" in the *Dll-1* locus resulted in β-galactosidase expression in endothelial cells [28]. In conclusion, we observe that *Serrate 1* is expressed with a topographic pattern very similar to that of *Notch 3*, while we cannot observe *Dll-1* expression in the postnatal brain.

Notch 3 Expression in the Human Fetal and Adult Brain

As *Notch 3* was expressed in both the pre- and postnatal mouse brain we wanted to learn whether this was true also for the human brain. By RT–PCR we could detect amplification of a fragment of the expected size for *Notch 3* from both fetal and adult human brain cDNA (Fig. 8). The identity of the PCR products was confirmed by hybridization with a probe corresponding to part of the amplified human *Notch 3* cDNA sequence (Fig. 8). We thus conclude that the *Notch 3* gene is expressed in both the fetal and adult human brain.

DISCUSSION

Our data show that the *Notch 3* gene is dynamically expressed during blood vessel development in the mouse brain and that the human *Notch 3* gene is expressed in both fetal and adult brain. During embryonic stages in the mouse, *Notch 3* expression is largely associated with cells in the walls of the major blood vessels of the head region (perineural vascular plexus) that eventually give rise to the carotid and other cranial arteries. Expression of the *Notch 3* gene is associated with small to medium-sized penetrating arteries in early postnatal stages and persists within these arteries even in the adult mouse brain. Furthermore, expression is restricted to small to medium-sized arteries and absent from small arterioles and capillaries. During development of the brain vasculature, the perineural vascular plexus is first formed before intracerebral vascularization [29]. Capillary sprouts originating from the perineural plexus subsequently penetrate into the brain tissue and establish a complex network of intracerebral blood vessels, a process that is accompanied by maturation of the vessel wall. In rodents, this step of brain angiogenesis is maximal in the early postnatal period. Therefore, *Notch 3* expression seems to be associated with mature or maturing rather than *de novo* forming (vasculogenic) blood vessels of the brain. It is also noticeable that *Notch 3* is expressed exclusively in arterial vessels but not in veins.

Several lines of evidence support the notion that *Notch 3* expression is localized to VSMCs. First, expression is seen in the vessel wall of prenatal arteries but not veins, which at this stage possess only a rudimentary smooth muscle cell coating. Second, staining is absent from capillaries. The finding that *Notch 3* expression during embryogenesis is localized to

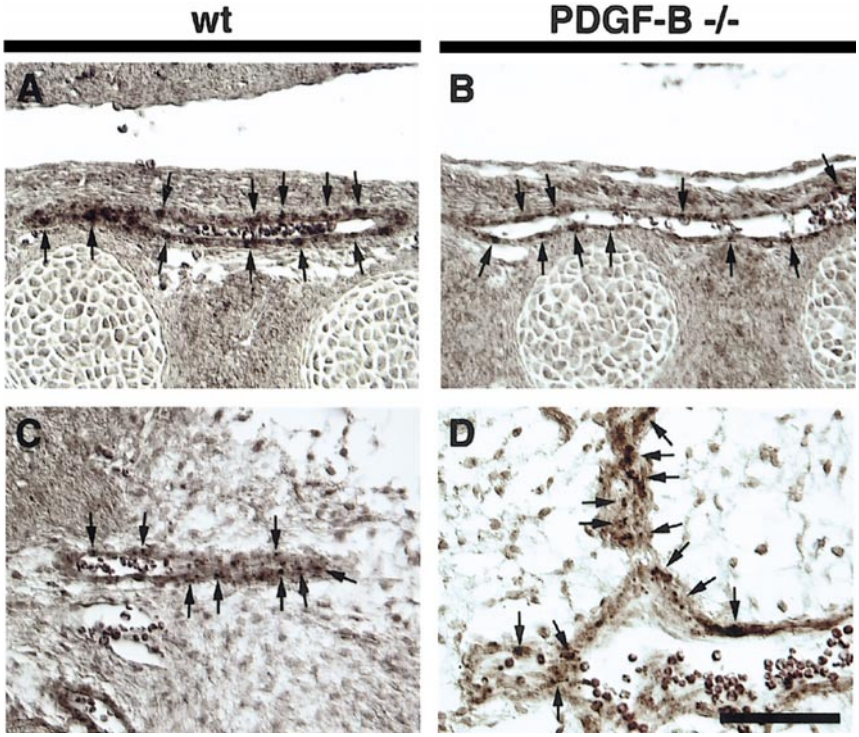

FIG. 6. Notch 3 expression is not altered in PDGF-B deficient mice. The staining pattern (arrows) observed for Notch 3 in the wall of body (A and B) or cranial (C and D) arteries after hybridization of a Dig-labeled antisense probe is similar in both a PDGF-B$-/-$ mouse embryo (B and D) and its wild-type littermate (A and C) at E14.5. However, the intensity of the stain within the body artery wall is somewhat reduced in the knock-out embryo (B), probably reflecting a diminished VSMC layer around this vessel. Scale bar: 100 μm.

VSMCs in aorta and larger vessels in the perineural vascular plexus, but not to forming capillaries, receives support from the analysis of expression in PDGF-B-deficient embryos. In these embryos, the larger vessels of the perineural vascular plexus still retain some VSMCs, while there is a near-complete loss of α-SMA-positive pericytes/VSMCs around capillaries in the brain. The fact that *Notch 3*-expressing cells exist although at somewhat reduced numbers indicates that they are localized in larger vessels, but not along capillaries. Third, *Notch 3* expression, at both the mRNA and protein levels, appears to be confined to cells juxtaposed to cells lining the vessel wall, but not to cells immediately adjacent to the vessel lumen. Fourth, the *Notch 3* expression pattern correlates with immunocytochemical staining for α-SMA but not for the endothelial marker PECAM-1. The confinement of *Notch 3* expression to VSMCs in the mouse is in keeping with recent data from human control and CADASIL brains, where immunostaining for *Notch 3* was seen in VSMCs [19]. Moreover, Leimeister *et al.* [25] recently localized mouse *Notch 3* mRNA expression to VSMCs in blood vessels of an embryonic day 14.5 embryo. Finally, our data suggest that only a scattered subpopulation of VSMCs express *Notch 3,* as the number of α-SMA expressing cells in comparable vessel segments nearly always exceeds the number of *Notch 3*-expressing cells. Taken together, the data presented here and the recent data from human brains [19] demonstrate an evolutionary conservation in *Notch 3* expression between mouse and humans. This suggests that the mouse can be used as an experimental model system to analyze by transgenic experiments how the specific *Notch 3* mutations lead to a CADASIL-like pathology.

We find that one of the *Notch* ligands, *Serrate 1,* but not *Dll-1,* is expressed in a scattered subset of VSMCs, similar to the *Notch 3* pattern. The proximity to Serrate 1-expressing cells suggests that in VSMCs, the *Notch 3* receptor may be activated by *Serrate 1*. The recent finding that the *Serrate 1* ligand interacts with very high affinity with the *Notch 3* receptor *in vitro* may support this notion [30]. An interesting possibility is therefore that *Notch 3* and *Serrate 1* are expressed in alternating cells within the arterial vessel wall and interact with each other in a signaling pathway. Since Notch ligand-receptor signaling depends on direct cell–cell interaction, signaling between VSMCs is an attractive possibility. Furthermore, differential expression of *Notch* ligands and receptors in an otherwise homogenous cell population is typical for lateral inhibition [18], as seen, for example, in inner ear development [31]. The importance of *Serrate 1* expression for cranial

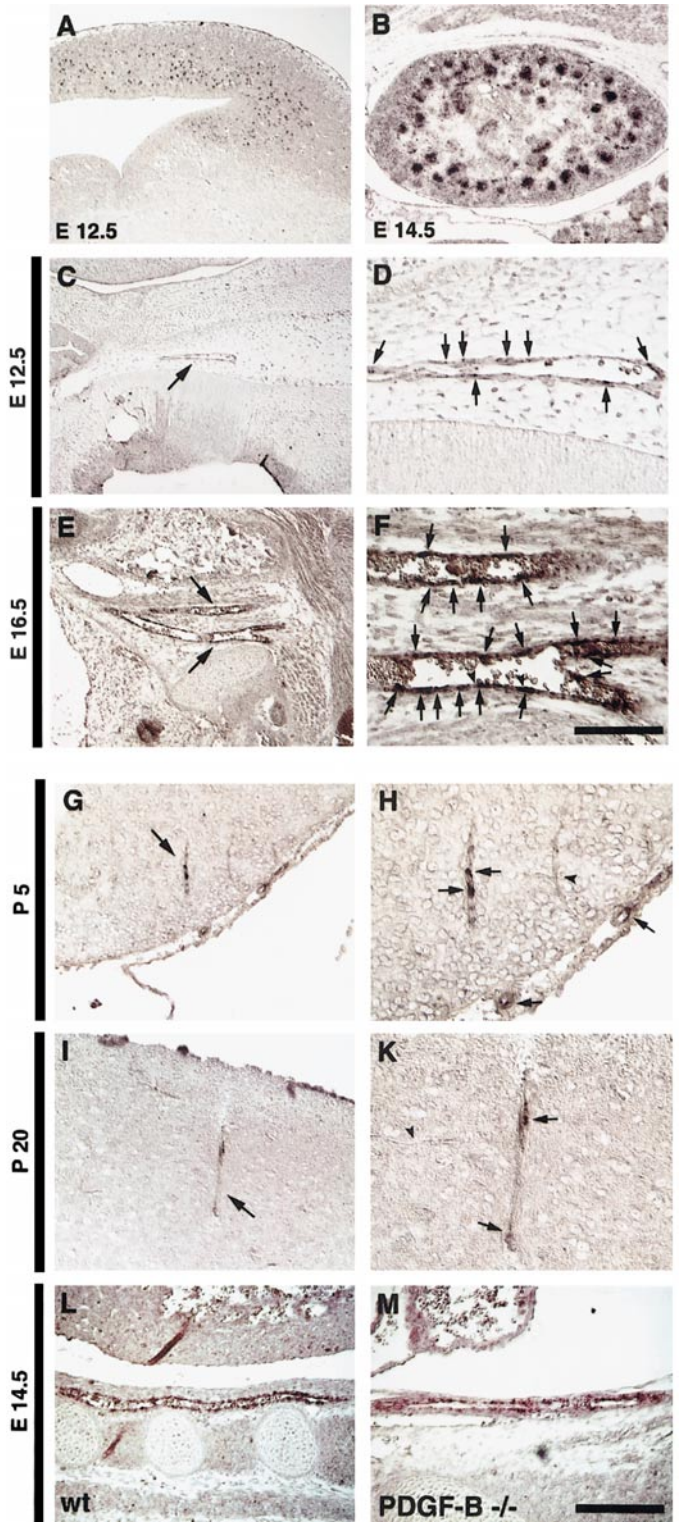

FIG. 7. Mouse *Serrate-1* is expressed in a subset of vascular mural cells in a similar pattern as *Notch 3*. Sagittal sections of E12.5 (A, C, and D), E14.5 (B, L, and M), and E16.5 (E and F) mouse embryos, and coronal sections of P5 (G and H) and P20 (I and K) mouse brains. After hybridization of a Dig-labeled mSerrate-1 antisense riboprobe and subsequent enzymatic detection using an anti-Dig/alkaline phospatase-conjugated antibody and NBT/BCIP as color substrate, scattered cells expressing *Serrate-1* are detected in the midbrain region of an E12.5 mouse embryo (A) and an intense staining is seen in the glomeruli of the kidney at E14.5 (B). (D) Higher magnification of a major blood vessel from the perineural vascular plexus at E12.5 (arrow in C) or branching vessels (F) in the head region of an E16.5 embryo (arrows in E) reveals that *Serrate-1* expression is confined to a subpopulation of cells within the vessel wall (arrows in D and F), while morphologically distinct endothelial cells are not stained (arrowheads in F). In the postnatal mouse brain, *Serrate-1* expression is confined to small to medium-sized penetrating arteries in superficial cortical areas (arrows in G and I) and appears to be associated with the vessel wall (arrows in H and K). Note that not all similarly sized penetrating arteries in the vicinity of the marked vessel are stained (arrowhead in H), and capillaries in close proximity to the stained vessel also remain unstained (arrowhead in K). *Serrate-1* expression appeared not to be altered in an E14.5 PDGF-B-deficient embryo (M), compared to a wild-type littermate (L). Scale bar: 400 μm (A, B, C, and E), 100 μm (D, F, H, and K), 150 μm (Land M), and 200 μm (G and I).

blood vessel development has recently been demonstrated in mice lacking the mouse *Jagged (Serrate) 1* gene [32]. These cranial vessels show an abnormal appearance and reduced diameter and appear to be the first site of hemorrhage in the homozygous mutant embryos, suggesting severe defects in angiogenic vascular remodeling. In addition to *Serrate 1*, the recently discovered *Notch* ligand *Dll-4* may be a potential ligand, since it is expressed in the endothelium of the arterial system [33]. During early embryogenesis, *Dll-4* is implicated as a ligand for *Notch 1* and *Notch 4*, since mouse embryos lacking both *Notch 1* and *4* displayed severe defects in angiogenic vascular remodeling at sites where *Dll-4* is expressed [33].

Notch 3 and CADASIL

The localization of postnatal *Notch 3* expression to the small to medium-sized arteries, and presumably to a subset of VSMCs, in the mouse brain presented here and to VSMCs in human adult brain [19] has important implications for the understanding of the pathogenesis of CADASIL. First, analysis of brain biopsies from CADASIL patients reveals that subcortical and meningial small and medium-sized cerebral arteries of the brain are the primary site of pathological alterations [7]. The affected blood vessels exhibit a narrowing of the lumen and a notorious thickening of the vessel wall, while the surrounding brain tissue shows evidence of edema, gliosis, and demyelination that may be caused by chronic hypoperfusion through the stenotic blood vessels (for review see [34]). The finding that *Notch 3* expression correlates with the site of pathogenesis further underlines the genetic link between *Notch 3* and CADASIL and demonstrates that the effects of CADASIL mutations are confined to the region in which *Notch 3* is expressed.

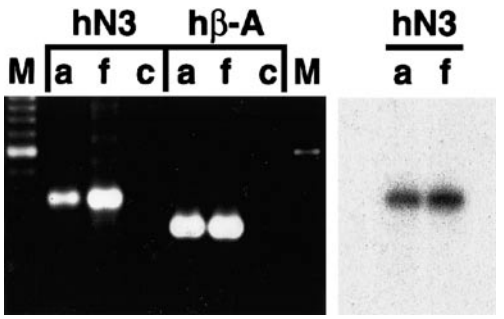

FIG. 8. Human *Notch 3* is expressed in both fetal and adult human brain. Amplification of a 401-bp fragment after reverse transcription of human adult (a) and fetal (f) poly(A)$^+$ RNA corresponding to human *Notch 3* (hN3) and of a 308-bp fragment corresponding to human β-actin (hβ-A) from adult (a) and fetal (f) human brain (as positive control). Both PCR reactions were run using the same cycling parameters. (M) The 100-bp size standard (the bright band corresponds to 600 bp); (c) water controls. The identity of the amplified human *Notch 3* fragments was confirmed by hybridization of the blotted bands with a 48-mer corresponding to part of the amplified sequence from human *Notch 3* for both adult (a) and fetal (f) human brain.

Second, the expression data shed light on which vascular cell type is primarily affected in CADASIL. A wealth of genetic and biochemical data show that *Notch* receptor function is cell autonomous (for review see [18]). *Notch 3* expression in VSMCs therefore strongly suggests that these cells are the primary targets in CADASIL and that the changes in endothelial cells and in the white matter observed in CADASIL patients are secondary to the pathological alterations in VSMCs. This view is supported by the temporal sequence of vascular cell changes in CADASIL. The first changes observed at the ultrastructural level in the affected arteries are the accumulation of GOM in the extracellular space in close proximity to VSMCs exhibiting an altered morphology or often within the thickened or reduplicated VSMC basement membrane [7, 35, 36]. The affected VSMCs often show multiple infoldings of the cell membrane harboring GOM [35, 36]. Furthermore, the presence of an increased number of pinocytotic vesicles along the cell membrane of affected VSMCs opposite to GOM deposits has been reported in several cases [35, 36]. These findings suggest that GOM may be derived from the VSMCs, as a consequence of expression of a mutated *Notch 3* receptor.

How do mutations in the *Notch 3* gene lead to the pathological changes in VSMCs? CADASIL is a dominant, highly penetrant disease. All known CADASIL mutations generate EGF-repeats with an odd number of cysteine residues, presumably leading to an unpaired cysteine residue in the extracellular domain of the mutated receptor [13]. Molecular modeling of EGF repeats from *Notch 3* indicates that CADASIL mutations will lead to domain misfolding [5]. A number of possible molecular explanations for CADASIL can be proposed. First, CADASIL mutations may result in a hyper- or hypoactive receptor. In this context, it is interesting to observe that the intracellular domain of the *Notch 3* receptor has an effect which is different from other characterized *Notch* receptors and in fact represses *Notch 1*-mediated activation in both developing CNS and pancreas [16, 17]. Increased activity of the *Notch 3* receptor may therefore lead to a reduction of *Notch 1*-mediated signaling, and conversely, reduced *Notch 3* activity could enhance the activity of *Notch 1*, for example, by elevating HES gene expression.

Second, the intracellular processing and/or trafficking of the mutated receptor could be altered in the VSMCs, possibly as a result of altered protein conformation. Indeed, in protein extracts from CADASIL brains, an accumulation of the *Notch 3* ectodomain is observed [19]. Furthermore, the accumulation of GOM in close association to the affected VSMCs may support this notion. Although the biochemical nature of these deposits is still unknown, it can be excluded that they contain amyloid, immunoglobulins, or metallic and mineral components [8]. It is interesting to observe that *Notch 3* immunoreactivity was not found in GOMs, but rather in the vicinity, at the VSMC plasma membrane [19].

Third, the impaired cysteine residue may promote an aberrant interaction of the mutated *Notch 3* receptors with another *Notch 3* receptor or with other cysteine-rich proteins at the cell surface. Evidence for high-molecular-weight protein complexes containing *Notch 3* from CADASIL brains was recently presented [19]. VSMCs play a pivotal role in the production and organization of a specialized extracellular matrix (ECM), which is required for the proper formation of a multilayered vessel wall in arteries [37]. One intriguing possibility to explain why the CADASIL *Notch 3* mutations are pathogenic in brain arteries, but not at other sites of expression during early embryogenesis [10, 21, 26], would be to propose a specific interaction between *Notch 3* and a protein unique to the specialized arterial ECM. If such an interaction would involve an ECM protein appearing only at later developmental stages, as a consequence of remodeling the ECM during development [37], it may provide an explanation for the late onset of the disease. Alternatively, the GOM is only slowly built up over time, and a long and continuous period of *Notch 3* expression is a prerequisite for the onset of the disease. It should also be noted that the CADASIL-affected arteries in the brain are of the end artery type and occlusion leads to infarct, whereas in many other organs the collateral supply is sufficient to prevent ischemia (for review see [6]). Further work on *Notch 3* signaling and function in VSMCs in both cellular and transgenic systems is likely to shed more light on the molecular aspects of CADASIL.

We thank Dr. Hannu Kalimo for valuable comments on the article, Marie-Louise Spångberg for excellent technical assistance in the histology work, and Dr. Ulf Eriksson for the generous gift of antisera to PECAM-1 and advice on the immunohistochemistry. The work was supported by grants from Cancerfonden, Karolinska Institutet, AMF sjukförsäkrings Jubileumsstiftelse, Tore Nilsons Stiftelse, and a postdoctoral fellowship from the German Academic Exchange Service (DAAD) to N.P.

REFERENCES

1. Sourander, P., and Wålinder, J. (1977). Hereditary multi-infarct dementia. *Acta Neuropathol.* **39,** 247–254.
2. Tournier-Lasserve, E., Joutel, A., Melki, J., Weissenbach, J., Lathrop, G. M., Chabriat, H., Mas, J.-L., Cabanis, E.-A., Baudrimont, M., Maciazek, J., Bach, M.-A., and Bousser, M.-G. (1993). Cerebral autosomal dominant arteriopathy with subcortical infarcts and leukoencephalopathy maps to chromosome 19q12. *Nat. Genet.* **3,** 256–259.
3. Joutel, A., Corpechot, C., Ducros, A., Vahedi, K., Chabriat, H., Mouton, P., Alamowitch, S., Domenga, V., Cécillion, M., Maréchal, E., Maciazek, J., Vayssière, E., Cruaud, C., Cabanis, E.-A., Ruchoux, M. M., Weissenbach, J., Bach, J. F., Bousser, M. G., and Tournier-Lasserve, E. (1996). *Notch3* mutations in CADASIL, a hereditary adult-onset condition causing stroke and dementia. *Nature* **383,** 707–710.
4. Chabriat, H., Vahedi, K., Iba-Zizen, M. T., Joutel, A., Nibbio, A., Nagy, T. G., Krebs, M. O., Julien, J., Dubois, B., Ducrocq, X., Levasseur, M., Homeyer, P., Mas, J. L., Lyon-Caen, O., Tournier-Lasserve, E., and Bousser, M. G. (1995). Clinical spectrum of CADASIL: A study of 7 families. *Lancet* **346,** 934–939.
5. Dichgans, M., Mayer, M., Uttner, I., Bruning, R., Muller-Hocker, J., Rungger, G., Ebke, M., Klockgether, T., and Gasser, T. (1998). The phenotypic spectrum of CADASIL: Clinical findings in 102 cases. *Ann. Neurol.* **44,** 731–739.
6. Kalimo, H., Viitanen, M., Amberla, K., Juvonen, V., Marttila, R., Pöyhönen, M., Rinne, J. O., Savontaus, M.-L., Tuisku, S., and Winblad, B. (1999). CADASIL: Hereditary disease of arteries causing brain infarcts and dementia. *Neuropath. Appl. Neurobiol.* **25,** 257–265.
7. Ruchoux, M.-M., Guerouaou, D., Vandenhaute, B., Pruvo, J.-P., Vermersch, P., and Leys, D. (1995). Systemic vascular smooth muscle cell impairment in cerebral autosomal dominant arteriopathy with subcortical infarcts and leukoencphalopathy. *Acta Neuropathol.* **89,** 500–512.
8. Ruchoux, M.-M., and Maurage, C.-A. (1998). Endothelial changes in muscle and skin biopsies in patients with CADASIL. *Neuropath. Appl. Neurobiol.* **24,** 60–65.
9. Larsson, C., Lardelli, M., White, I., and Lendahl, U. (1994). The human NOTCH 1, 2 and 3 genes are located at chromosome positions 9q34, 1p13-p11 and 19p13.2-13.1 in regions of neoplasia-associated translocation. *Genomics* **24,** 253–258.
10. Lardelli, M., Dahlstrand, J., and Lendahl, U. (1994). The novel *Notch* homologue mouse *Notch 3* lacks specific EGF-repeats and is expressed in proliferating neuroepithelium. *Mech. Dev.* **46,** 123–136.
11. Gridley, T. (1997). Notch signaling in vertebrate development and disease. *Mol. Cell. Neurosci.* **9,** 103–108.
12. Beatus, P., and Lendahl, U. (1998). Notch and neurogenesis. *J. Neurosci. Res.* **54,** 125–136.
13. Joutel, A., Vahedi, K., Corpechot, C., Troesch, A., Chabriat, H., Vayssiére, C., Cruaud, C., Maciazek, J., Weissenbach, J., Bousser, M.-G., Bach, J.-F., and Tournier-Lasserve, E. (1997). Strong clustering and stereotyped nature of *Notch3* mutations in CADASIL patients. *Lancet* **350,** 1511–1515.
14. Dichgans, M., Ludwig, H., Müller-Höcker, J., Messerschmidt, A., and Gasser, T. (2000). Small in-frame deletions and missense mutations in CADASIL: 3D models predict misfolding of Notch3 EGF-like repeat domains. *Eur. J. Hum. Gen.* **8,** 280–285.
15. Lewis, J. (1998). A short cut to the nucleus. *Nature* **393,** 304–305.
16. Beatus, P., Lundkvist, J., Öberg, C., and Lendahl, U. (1999). The Notch 3 intracellular domain represses Notch 1-mediated activation through Hairy/Enhancer of split (HES) promoters. *Development* **126,** 3925–3935.
17. Apelqvist, Å., Li, H., Sommer, L., Beatus, P., Anderson, D. J., Honjo, T., Hrabe de Angelis, M., Lendahl, U., and Edlund, H. (1999). Notch signalling controls pancreatic cell differentiation. *Nature* **400,** 877–881.
18. Simpson, P. (1997). Notch signalling in development: On equivalence groups and asymmetric developmental potential. *Curr. Op. Gen. Dev.* **7,** 537–542.
19. Joutel, A., Andreux, F., Gaulis, S., Domenga, V., Cecillon, M., Battail, N., Piga, N., Chapon, F., Godfrain, C., and Tournier-Lasserve, E. (2000). The ectodomain of the Notch 3 receptor accumulates within the cerebrovasculature of CADASIL patients. *J. Clin. Invest.* **105,** 597–605.
20. Hellström, M., Kalén, M., Lindahl, P., Abrahamsson, A., and Betsholtz, C. (1999). Role of PDGF-B and PDGFR-β in recruitment of vascular smooth muscle cells and pericytes during embryonic blood vessel formation in the mouse. *Development* **126,** 3047–3055.
21. Mitsiadis, T. A., Henrique, D., Thesleff, I., and Lendahl, U. (1997). Mouse *Serrate-1* (*Jagged-1*): Expression in the developing tooth is regulated by epithelial-mesenchymal interactions and fibroblast growth factor-4. *Development* **124,** 1473–1483.
22. Lindahl, P., Johansson, B. R., Levéen, P., and Betsholtz, C. (1997). Pericyte loss and microaneurysm formation in PDGF-B-deficient mice. *Science* **277,** 242–245.
23. Maniatis, T., Fritsch, E. F., and Sambrook, J. (1989). "Molecular Cloning: A Laboratory Manual," Cold Spring Harbor Laboratory, Cold Spring Harbor, New York.
24. Mitsiadis, T. A., Lardelli, M., Lendahl, U., and Thesleff, I. (1995). Expression of *Notch 1, 2* and *3* is regulated by epithelial-mesenchymal interactions and retinoic acid in the developing mouse tooth and associated with determination of ameloblast cell fate. *J. Cell Biol.* **130,** 407–418.
25. Leimeister, C., Schumacher, N., Steidl, C., and Gessler, M. (2000). Analysis of HeyL expresion in wild-type and Notch pathway mutant mouse embryos. *Mech. Dev.* **98,** 175–178.
26. Lindsell, C. E., Boutler, J., diSibio, G., Gossler, A., and Weinmaster, G. (1996). Expression patterns of Jagged, Delta 1, Notch 1, Notch 2 and Notch 3 genes identify ligand-receptor pairs that may function in neural development. *Mol. Cell. Neurosci.* **8,** 14–27.
27. Bettenhausen, B., Hrabé de Angelis, M., Simon, D., Guénet, J.-L., and Gossler, A. (1995). Transient and restricted expression during mouse embryogenesis of Dll1, a murine gene closely related to *Drosophila* Delta. *Development* **121,** 2407–2418.
28. Beckers, J., Clark, A., Wünsch, K., Hrabé de Angelis, M., and Gossler, A. (1999). Expression of the mouse Delta1 gene during organogenesis and fetal development. *Mech. Dev.* **84,** 165–168.
29. Plate, K. H. (1999). Mechanisms of angiogenesis in the brain. *J. Neuropathol. Exp. Neurol.* **58,** 313–320.
30. Shimizu, K., Chiba, S., Kumano, K., Hosoya, N., Takahashi, T., Kanda, Y., Hamada, Y., Yazaki, Y., and Hirai, H. (1999). Mouse

Jagged 1 physically interacts with Notch 2 and other Notch receptors. *J. Biol. Chem*. **274,** 32961–32969.

31. Adam, J., Myat, A., Le Roux, I., Eddison, M., Henrique, D., Ish-Horowicz, D., and Lewis, J. (1998). Cell fate choices and the expression of Notch, Delta and Serrate homologues in the chick inner ear: Parallels with *Drosophila* sense-organ development. *Development* **125,** 4645–4654.
32. Xue, Y., Gao, X., Lindsell, C. E., Norton, C. R., Chang, B., Hicks, C., Gendron-Maguire, M., Rand, E. B., Weinmaster, G., and Gridley, T. (1999). Embryonic lethality and vascular defects in mice lacking the Notch ligand Jagged 1. *Hum. Mol. Gen.* **8,** 723–730.
33. Krebs, L. T., Xue, Y., Norton, C. R., Shutter, J. R., Maguire, M., Sundberg, J. P., Gallahan, D., Closson, V., Kitajewski, J., Callahan, R., Smith, G. H., Stark, K. L., and Gridley, T. (2000). Notch signaling is essential for vascular morphogenesis in mice. *Genes Dev*. **14,** 1343–1352.
34. Salloway, S., and Hong, J. (1998). CADASIL syndrome: A genetic form of vascular dementia. *J. Geriatr. Pshychiat. Neurol.* **11,** 71–77.
35. Mayer, M., Straube, A., Bruening, R., Uttner, I., Pongratz, D., Gasser, T., Dichgans, M., and Müller-Höcker, J. (1999). Muscle and skin biopsies are a sensitive diagnostic tool in the diagnosis of CADASIL. *J. Neurol.* **246,** 526–532.
36. Schultz, A., Santoianni, R., and Hewan-Lowe, K. (1999). Vasculopathic changes of CADASIL can be focal in skin biopsies. *Ultrastruc. Pathol.* **23,** 241–247.
37. Hungerford, J. E., and Little, C. D. (1999). Developmental biology of the vascular smooth muscle cell: Building a multilayered vessel wall. *J. Vasc. Res.* **36,** 2–27.
38. Williams, R., Lendahl, U., and Lardelli, M. (1995). Complementary and combinatorial patterns of *Notch* gene family expression during early mouse development. *Mech. Dev*. **53,** 357–368.

Received December 13, 2001
Revision received March 22, 2002
Published online June 20, 2002